







# Gigabit per second visible light communication based on AlGaInP red micro-LED micro-transfer printed onto diamond and glass

J. F. C. CARREIRA,<sup>1,3</sup>  E. XIE,<sup>1,4</sup>  R. BIAN,<sup>2</sup> J. HERRNSDORF,<sup>1</sup>  H. HAAS,<sup>2</sup>  E. GU,<sup>1,5</sup> M. J. STRAIN,<sup>1</sup>  AND M. D. DAWSON<sup>1</sup> 

<sup>1</sup>*Institute of Photonics, Department of Physics, University of Strathclyde, Glasgow G1 1RD, UK*

<sup>2</sup>*Institute for Digital Communications, Li-Fi R&D Centre, University of Edinburgh, Edinburgh EH9 3JL, UK*

<sup>3</sup>*jose.correia-carreira@strath.ac.uk*

<sup>4</sup>*enyuan.xie@strath.ac.uk*

<sup>5</sup>*erdan.gu@strath.ac.uk*

**Abstract:** Full-color smart displays, which act both as a display and as a high-speed visible light communication (VLC) transmitter, can be realized by the integration of red-green-blue micron-sized light emitting diodes (micro-LEDs) onto a common platform. In this work, we report on the integration of aluminum gallium indium phosphide red micro-LEDs onto diamond and glass substrates by micro-transfer printing and their application in VLC. The device on-diamond exhibits high current density and bandwidth operation, enabled by diamond's superior thermal properties. Employing an orthogonal frequency division multiplexing modulation scheme, error-free data rates of 2.6 Gbps and 5 Gbps are demonstrated for a single micro-LED printed on-glass and on-diamond, respectively. In a parallel configuration, a 2x1 micro-LED array achieves error-free data rates of 3 Gbps and 6.6 Gbps, on-glass and on-diamond, respectively.

Published by The Optical Society under the terms of the [Creative Commons Attribution 4.0 License](https://creativecommons.org/licenses/by/4.0/). Further distribution of this work must maintain attribution to the author(s) and the published article's title, journal citation, and DOI.

## 1. Introduction

Micron-sized light emitting diodes (micro-LEDs or  $\mu$ LEDs) are expected to become the next-generation of self-emissive displays and microdisplays [1]. Full-color micro-LED displays have been realized by mass transfer techniques, such as micro-transfer printing (micro-TP or  $\mu$ TP), of red-green-blue (RGB) singulated chiplets onto a common platform [2,3]. Blue and green pixels are fabricated from indium gallium nitride (InGaN) alloys grown on sapphire or silicon substrates [4]. Typically, the red emission is based on aluminum gallium indium phosphide (AlGaInP) LED structures grown on gallium arsenide (GaAs) [5,6]. These inorganic micron-sized pixels exhibit exceptional brightness, contrast and low power consumption. In addition, due to their smaller device capacitance and current density dependent differential carrier lifetime, micro-LEDs show extremely high modulation bandwidth, supporting visible light communication (VLC) up to several gigabits per second (Gbps) [7]. This opens the possibility for smart micro-LED displays acting both as a display and as a high-speed VLC transmitter [8].

In the past years, several demonstrations of Gbps VLC, employing spectrally efficient modulation schemes (such as, orthogonal frequency division multiplexing - OFDM) and GaN-based micro-LEDs (with emission wavelengths covering from the violet to the green) were reported [9–11]. In particular, nonpolar GaN-based micro-LEDs hold great promise for VLC applications, due to their extremely high bandwidth at low current density [12]. However, the internal polarization field effects of nitrides are not prevalent in AlGaInP/GaAs red LEDs, and, to

the best of our knowledge, there are no reports on data transmission capability of AlGaInP LEDs in micro-LED geometries. In this paper, we report on the integration of AlGaInP micro-LEDs onto glass and diamond substrates by micro-TP. The superior thermal properties of diamond over glass are evidenced by ability of the red micro-LED on-diamond to support higher current density, thus achieving 100's MHz of modulation bandwidth. In a free-space VLC link Gbps error-free data rates are demonstrated by both on-diamond and on-glass micro-LED devices. The broader implication of this work include application of these red micro-LED devices with polymer optical fibers and/or high turbidity underwater wireless optical communication systems.

## 2. Device fabrication by micro-TP

In this work, free-standing red (630 nm) micro-LED platelets were printed onto glass and diamond substrates. The epitaxial structure of these red micro-LEDs follows that of conventional AlGaInP epistuctures grown on GaAs [13]. Fabrication of the micro-LED platelets started by processing the topside of the AlGaInP/GaAs wafer following typical microfabrication procedures for mesa type LEDs. First, a  $6.96 \times 10^{-6} \text{ cm}^2$  active area pixel was defined by dry etching, exposing the  $n$  layer, followed by deposition of AuGe/Au and Ti/Al/Ti/Au metal stacks on the  $n$  and  $p$  contacts, respectively. Next, the GaAs wafer was flip-chip bonded to a temporary sapphire carrier and the GaAs bulk substrate removed by wet chemical etching [14]. Finally, the platelet was defined through the backside of the AlGaInP film by dry etching. Figure 1(a) shows a 2x2 array of micro-LED platelets on the temporary sapphire carrier.

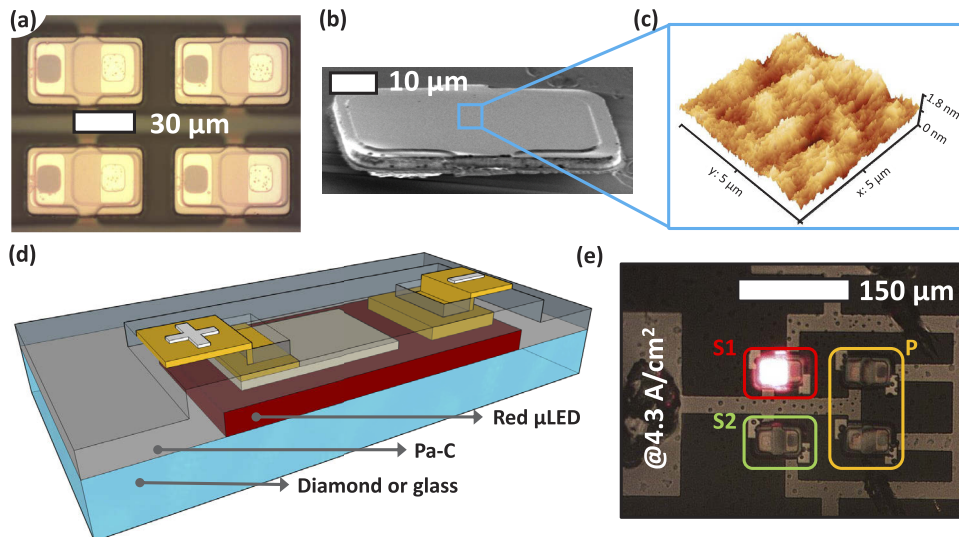


**Fig. 1.** (a) Plan-view photograph of a 2x2 array of micro-LED platelets on the temporary sapphire carrier; (b) scanning electron microscopy micrograph of a micro-LED platelet backside; (c) representative  $5 \times 5 \mu\text{m}^2$  atomic force microscopy micrograph of a micro-LED platelet backside; (d) schematic drawing of the transfer printed micro-LED after Parylene-C (Pa-C) encapsulation and metallization; (e) plan-view photograph of a finalised 2x2 micro-LED array printed onto glass with a single micro-LED (S1) driven at  $4.3 \text{ A/cm}^2$ .

Figure 1(b) shows a scanning electron microscopy (SEM) micrograph of a micro-LED platelet backside. The micro-LED platelet backside was found to be extremely flat, which can be attributed to the lattice matched and strain-free epitaxial growth of these LED structures on GaAs [5]. In addition, due to the high etching selectivity between the GaAs and the etch stop layer, the backside of the micro-LED platelet is extremely smooth, as shown by a representative  $5 \times 5 \mu\text{m}^2$

atomic force microscopy micrograph (Fig. 1(c)). The micro-LED platelet backside exhibits a root-mean-square (RMS) roughness of 0.2 nm, approaching the instrument resolution. The flatness and smoothness of the micro-LED platelet backside are important factors for micro-TP applications, as they improve the adhesion between the platelet and the receiving substrate. Furthermore, the good contact between the micro-LED platelet and the receiving substrate ensures efficient heat transfer.

A 2x2 array of micro-LEDs was sequentially printed directly, without any adhesion enhancement layer, onto glass and diamond substrates. The glass and single-crystal (synthetic) diamond substrates had the same dimensions, namely area 4x4 mm<sup>2</sup> and thickness 500 μm. An elastomeric polydimethylsiloxane (PDMS) stamp, with pyramidal protrusions, was used to pick-up the micro-LED platelets from the temporary sapphire carrier and print them onto both substrates [15]. The micro-LED platelets are bonded to the temporary sapphire carrier by a weak adhesive interlayer, which was optimized to allow retrieval of the platelets with the PDMS stamp. Due to PDMS viscoelastic properties, quick retraction of the stamp results in an adhesion strength between the micro-LED platelet and the stamp larger than the adhesion strength between the platelet and the weak adhesion interlayer; thus the micro-LED platelet is retrieved. On the other hand, when in contact with the receiving substrate, slow retraction of the stamp results in an adhesion strength between the platelet and the stamp smaller than the one between the platelet and the receiving substrate; thus the platelet is released [16]. After micro-TP, a Parylene-C (Pa-c) layer (thickness 4 μm) was deposited as an insulation and encapsulation layer. Next, Ti/Au (thicknesses 100/200 nm) metal tracks were lithographically defined, contacting the micro-LEDs through, previously defined by reactive ion etching, localized apertures in the Pa-C layer. Using lithographically processed electrical contacts allows efficient planar registration of the transfer printed micro-LEDs, without pre-processing the receiving substrate. In addition, this method can be easily extended to a variety of substrates, such as flexible polymers [17]. Figure 1(d) shows a schematic drawing of the transfer printed micro-LED after Pa-C encapsulation and metallization. The 2x2 array was arranged in order to have two individually addressable single micro-LEDs (identified in Fig. 1(e) as S1 and S2) and a 2x1 in-parallel micro-LED array (identified in Fig. 1(e) as P). Figure 1(e) shows the single micro-LED S1 driven at 4.3 A/cm<sup>2</sup>. It was found experimentally that the micro-LEDs S1 and S2 exhibit the same electrical and optical properties, on both substrates. Thus, for clarity sake, the device performance and application results are only shown for the micro-LED S1.

### 3. Device performance and application

#### 3.1. Micro-LED electrical, optical, and bandwidth characteristics

Figure 2(a) shows the current density vs voltage (JV) and current density vs optical power density (JL) of the single micro-LED S1 on-diamond and on-glass. The JV characteristic was measured by a voltage source, through scanning each data point under direct current (DC) conditions (Yokogawa GS610). The JL characteristic was measured using a calibrated Si photodiode detector (Thorlabs PM100D) placed in close proximity to the micro-LED backside. The forward diode voltage (at 32 A/cm<sup>2</sup>) of the single micro-LED on-diamond and on-glass was found to be 2.2 V and 2.1 V, respectively. The red micro-LED on-glass optical power density reaches a plateau of 16.6 W/cm<sup>2</sup> at 359 A/cm<sup>2</sup>. Due to diamond's superior thermal conductivity properties ( $k = 2200$  W/m.K) over glass ( $k = 1.42$  W/m.K) [18] the micro-LED on-diamond sustains current densities up to 790 W/cm<sup>2</sup> without any thermal roll-over. At the current density of 790 A/cm<sup>2</sup> the micro-LED on-diamond exhibits a near chip face optical power density of 39 W/cm<sup>2</sup> (more than twofold increase compared to the micro-LED on-glass).

The -6 dB electrical modulation bandwidth of the single micro-LED S1 on different substrates was measured by applying a DC bias combined with a small-signal modulation from an HP8753ES network analyzer. The optical response was lens-focused onto a silicon avalanche photodetector

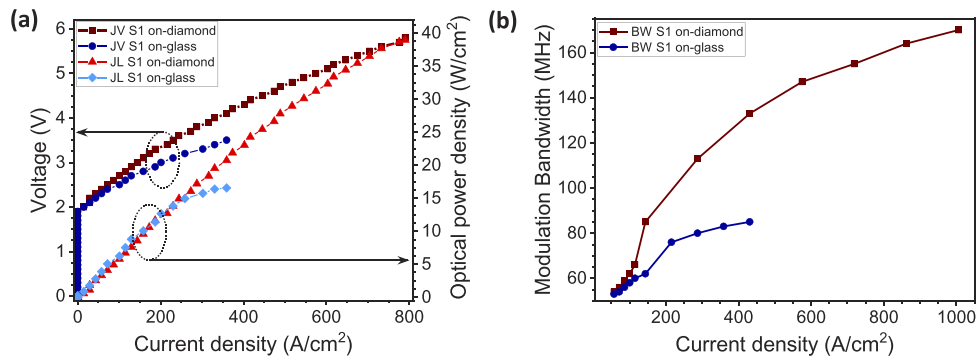


**Fig. 2.** (a) Current density vs voltage (JV) and current density vs optical power density (JL) curves of the single micro-LED S1 on-diamond and on-glass; (b) -6 dB electrical modulation bandwidth of the single micro-LED S1 on both substrates.

(Thorlabs — APD430A2/M bandwidth 400 MHz). Figure 2(b) shows the -6 dB electrical modulation bandwidth vs current density of the single micro-LED S1 on-diamond and on-glass. Devices on both glass and diamond exhibit similar performance for current densities below 100 A/cm<sup>2</sup>. Above this point, the micro-LED on-glass exhibits a lower modulation bandwidth until it reaches a plateau of 85 MHz at 431 A/cm<sup>2</sup>. On the other hand, the micro-LED on-diamond modulation bandwidth continues to increase up to 170 MHz at 1000 A/cm<sup>2</sup>.

Figure 3(a) shows the electroluminescence (EL) spectra of the single micro-LED S1 driven at 359 A/cm<sup>2</sup> on both substrates. The inset in Fig. 3(a) shows the CIE1931 color coordinates of the single micro-LED S1 on both substrates on the color space chromaticity diagram. The EL spectra were acquired using an optical fiber-coupled spectrometer (Avantes AvaSpec-2048L spectrometer). Both spectra show fringes due to refractive index contrast between the LED epitaxial material ( $n=3.5$  [19]) and both substrates (glass  $n=1.46$  [20], diamond  $n=2.41$  [21]). The micro-LED on-diamond exhibits an EL peak centered at 631.8 nm and a full width at full maximum (FWHM) of 19 nm. While, the micro-LED on glass EL peak is red-shifted (peak emission centered at 634.5 nm) and broadened (FWHM = 22 nm) due to bandgap shrinkage

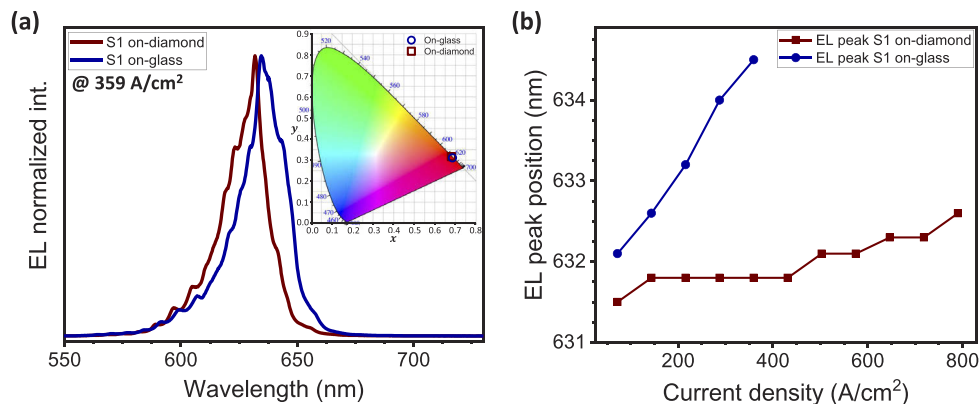


**Fig. 3.** (a) Electroluminescence (EL) spectra of the single micro-LED S1 (at 359 A/cm<sup>2</sup>) on both substrates (inset: CIE1931 color coordinates of the single micro-LED S1 on both substrates (at 359 A/cm<sup>2</sup>)); (b) EL spectra peak position vs current density of the single micro-LED S1 on both substrates.

and band filling effects, respectively. Nevertheless, these variations have a marginal effect on the perceived color, with the micro-LED on-diamond ( $x = 0.68, y = 0.32$ ) and on-glass ( $x = 0.69, y = 0.31$ ) showing similar  $(x, y)$  CIE1931 color coordinates. Figure 3(b) shows the EL peak position vs current density for the single micro-LED S1 printed on-diamond and on-glass. For the device on-glass, increasing the current density from  $72 \text{ A/cm}^2$  to  $359 \text{ A/cm}^2$  results in a steep red-shift of the peak position from  $632.1 \text{ nm}$  to  $634.5 \text{ nm}$  ( $\Delta\lambda = 2.4 \text{ nm}$ ). On the other hand, for the device on-diamond, under the same current density interval, the peak only red-shifts by  $0.3 \text{ nm}$ . In fact, due to diamond's excellent thermal conductivity varying the current density from  $72 \text{ A/cm}^2$  to  $790 \text{ A/cm}^2$  results in a red-shift from  $631.5 \text{ nm}$  to  $632.6 \text{ nm}$  ( $\Delta\lambda = 1.1 \text{ nm}$ ).

### 3.2. VLC application

Optical orthogonal frequency division multiplexing (O-OFDM) has proven to be spectrally efficient in VLC [22,23]. In this work, an implementation of direct current biased optical OFDM (DCO-OFDM) is used for the wireless data transmission due to its simplicity and high spectral efficiency [24]. As intensity modulation and direct detection (IM/DD) is used in VLC, the transmitted signal should be both real and non-negative. Thus Hermitian symmetry is applied and a DC bias is added.

A schematic drawing of the VLC experimental set-up is shown in Fig. 4. A random bit stream is encoded into an OFDM signal by MATLAB and then generated by an arbitrary waveform generator (AWG, Keysight M8195A). The analogue signal is amplified by a power amplifier (SHF S126A) and then combined with a DC bias (Yokogawa GS610) through a bias-tee (Tektronix PSPL5575A). The output of the bias-tee is connected to the micro-LED device. The link distance is set to  $40 \text{ cm}$ , as in this case we wish to assess the upper modulation limits of the devices, and aspheric condenser lenses (ACL4532A) have been used at both transmitter and receiver side. The optical signal is detected by a photoreceiver (Femto HSPR-X-I-1G4-SI). The output electrical signal is captured by an oscilloscope (Keysight DSA90804B) and then sent to the PC for processing using MATLAB.

Within each measurement, a channel estimation is first done to estimate the signal-to-noise ratio (SNR) at each subcarrier. Then the signal is generated using an adaptive bit and power loading algorithm based on the estimated SNR and a target bit-error-ratio (BER). Such signal is transmitted and the achieved data rate and BER are measured.

The VLC results of the red micro-LED devices on both substrates are summarized in Fig. 5. The DC bias and the modulation signal peak-to-peak voltage, after the amplifier, were set to  $359 \text{ A/cm}^2$  ( $862 \text{ A/cm}^2$ ) and  $2.68 \text{ V}$  ( $7.19 \text{ V}$ ), respectively, for the single micro-LED S1 on-glass (on-diamond). The sampling frequency was set at  $16 \text{ GSa/s}$  and the number of samples per symbol was optimized for each substrate. The estimated SNR and number of allocated bits, at the highest data rate below the FEC threshold of  $3.8 \times 10^{-3}$  BER, for the single micro-LED S1

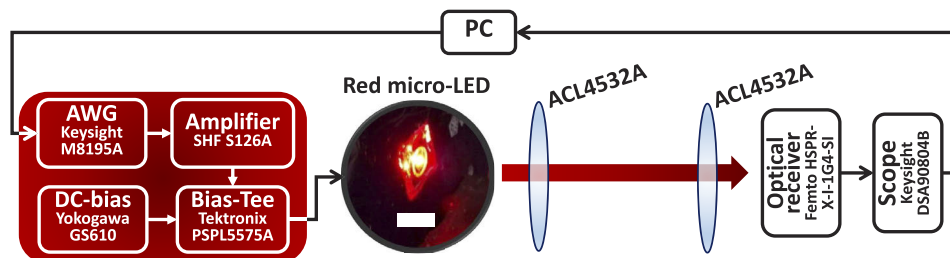


**Fig. 4.** Schematic diagram of the visible light communication experimental set-up. The photograph inset is the micro-LED on-diamond device (white scale bar corresponds to  $1 \text{ cm}$ ).



on-glass (blue curve and blue bar plot) and on-diamond (red curve and red bar plot) are shown in Fig. 5(a).

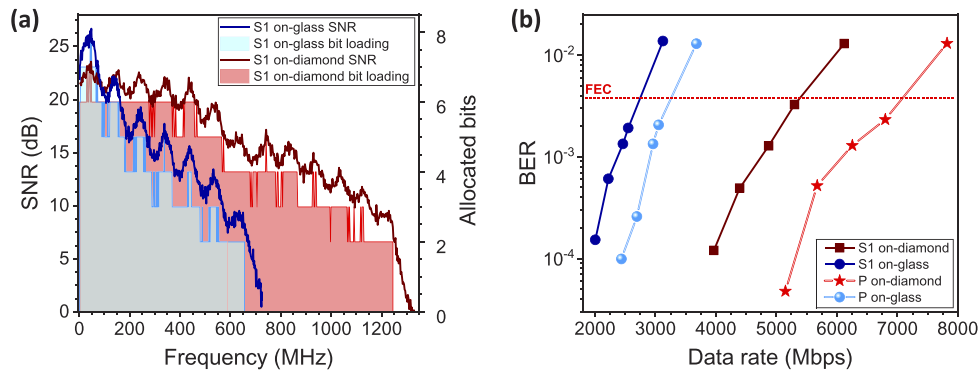


**Fig. 5.** (a) Signal-to-noise ratio and number of allocated bits (at maximum data rate below forward error correction) for the single micro-LED S1 on both substrates (glass and diamond); (b) bit-error-ratio (BER) vs data rate for the single micro-LED S1 and in-parallel micro-LED array P on both substrates.

As the micro-LED on-glass exhibits lower optical power and bandwidth its SNR suffers a sharp drop with frequency, supporting bit loading only up to 656 MHz. On the other hand, the micro-LED on-diamond higher optical power and bandwidth (due to its higher current density operation) results in a smooth decrease of the SNR with frequency and bit loading up to 1245 MHz. These differences in SNR and bit loading lead to the difference in BER vs data rate curves shown in Fig. 5(b). At the BER of  $3.8 \times 10^{-3}$  a single micro-LED on-glass achieves a data rate of 2749 Mbps, with the device on-diamond achieving 5391 Mbps (roughly a twofold increase). These results show the importance of efficient thermal management in LED-based VLC transmitters. Applying the 7% FEC overhead reduction, error-free data rates of 2557 Mbps and 5014 Mbps are achieved for the single micro-LED S1 on-glass and on-diamond, respectively. Also shown in Fig. 5(b) is the BER vs data rate performance of the 2x1 in-parallel micro-LED array P on both substrates. For this purpose, the DC bias and the modulation signal peak-to-peak voltage, after the amplifier, were set to 323 A/cm<sup>2</sup> (718 A/cm<sup>2</sup>) and 3.26 V (6.62 V), respectively, for the in-parallel micro-LED array on-glass (on-diamond). Although the current density is lower than a single micro-LED, the total optical power of the array is roughly two times higher than of a single micro-LED. This translates into an increase in SNR and capacity to allocate more bits to the in-parallel micro-LED arrays. Thus, the in-parallel micro-LED array on-glass achieves 3262 Mbps below FEC threshold (a 1.2x increase compared to its single counterpart). For the device transfer printed on-diamond a data rate of 7093 Mbps, below FEC, is achieved (a 1.3x increase compared to a single device on-diamond). Again, applying the 7% FEC overhead reduction, error-free data rates of 3034 Mbps and 6596 Mbps are obtained for the in-parallel micro-LED array on-glass and on-diamond, respectively.

Table 1 compares the data rate, BER, and link distance achieved by the single micro-LED S1 and by the in-parallel micro-LED array P on-diamond, with other red LED-based VLC reports from our previous work. The data rates achieved in this work are higher than the ones obtained using commercially available LEDs [25,27] or resonant cavity LEDs [26] employing similar modulation schemes. Due to the micro-LEDs lower optical power the link distance is shorter than for commercial LEDs. However, it has been shown that the optical power can be increased, without any penalty in modulation bandwidth, by simply arranging several micro-LEDs in-parallel or in-series configurations [28].

**Table 1. State-of-the-art of red LED-based VLC.**

Transmitter	Data rate (Mbps)	BER	Link distance (m)	Ref.
Micro-LED	5391 (S1)	$3.8 \times 10^{-3}$	0.4	This work
	7093 (P)			
Commercial LED	4904	$2.5 \times 10^{-3}$	1.6	[25]
Resonant cavity LED	4000	$3.4 \times 10^{-3}$	1.5	[26]

#### 4. Conclusion

In conclusion, we have demonstrated the integration of AlGaInP micro-LED platelets onto diamond and glass by micro-transfer printing, without any adhesion-enhancement layer. A single micro-LED printed onto diamond can be driven up to 790 A/cm<sup>2</sup> displaying an optical power of 39 W/cm<sup>2</sup> (more than two times the optical power density of the counterpart device on-glass). The ability of the device on-diamond to sustain higher current density allows to achieve modulation bandwidths up to 170 MHz (with the device on-glass plateauing at 85 MHz). The heat-spreading properties of the diamond substrate are supported by the marginal red-shift of 1.1 nm of the micro-LED emission with increasing current density. Error-free data rates of 5014 Mbps and 6596 Mbps are obtained for a single micro-LED and a 2x1 in-parallel micro-LED array transfer printed onto diamond, respectively. These data rates are the highest reported values in literature for red LED-based VLC.

This work benchmarks the application of AlGaInP micro-LEDs in VLC and paves the way towards full-color pixelated clusters in micro-LED displays operating as wavelength division multiplexing VLC transmitters. In addition, the devices reported in this work are of importance for data transmission in plastic optical fibers and/or in high-turbidity water media.

Supporting data is available at DOI: [10.15129/593ca4b1-1184-4b0f-8dd3-aa9c63382d6f](https://doi.org/10.15129/593ca4b1-1184-4b0f-8dd3-aa9c63382d6f).

#### Funding

Engineering and Physical Sciences Research Council (EP/R03480X/1, EP/S001751/1, EP/T00097X/1).

#### Disclosures

The authors declare no conflicts of interest.

#### References

1. T. Wu, C.-W. Sher, Y. Lin, C.-F. Lee, S. Liang, Y. Lu, S.-W. Huang, W. Guo, H.-C. Kuo, and Z. Chen, "Mini-LED and Micro-LED: Promising Candidates for the Next Generation Display Technology," *Appl. Sci.* **8**(9), 1557 (2018).
2. C. A. Bower, M. A. Meitl, B. Raymond, E. Radauscher, R. Cok, S. Bonafede, D. Gomez, T. Moore, C. Prevatte, B. Fisher, R. Rotzoll, G. A. Melnik, A. Fecioru, and A. J. Trindade, "Emissive displays with transfer-printed assemblies of 8  $\mu\text{m}$  x 15  $\mu\text{m}$  inorganic light-emitting diodes," *Photonics Res.* **5**(2), A23–A29 (2017).
3. Y. Li, J. Tao, Y. Zhao, J. Wang, J. Lv, Y. Qin, J. Liang, and W. Wang, "48x48 pixelated addressable full-color micro display based on flip-chip micro leds," *Appl. Opt.* **58**(31), 8383–8389 (2019).
4. G. Li, W. Wang, W. Yang, Y. Lin, H. Wang, Z. Lin, and S. Zhou, "GaN-based light-emitting diodes on various substrates: a critical review," *Rep. Prog. Phys.* **79**(5), 056501 (2016).
5. T. Gessmann and E. F. Schubert, "High-efficiency AlGaInP light-emitting diodes for solid-state lighting applications," *J. Appl. Phys.* **95**(5), 2203–2216 (2004).
6. J.-T. Oh, S.-Y. Lee, Y.-T. Moon, J. H. Moon, S. Park, K. Y. Hong, K. Y. Song, C. Oh, J.-I. Shim, H.-H. Jeong, J.-O. Song, H. Amano, and T.-Y. Seong, "Light output performance of red AlGaInP-based light emitting diodes with different chip geometries and structures," *Opt. Express* **26**(9), 11194–11200 (2018).
7. S. Rajbhandari, J. J. D. McKendry, J. Herrnsdorf, H. Chun, G. Faulkner, H. Haas, I. M. Watson, D. O'Brien, and M. D. Dawson, "A review of gallium nitride LEDs for multi-gigabit-per-second visible light data communications," *Semicond. Sci. Technol.* **32**(2), 023001 (2017).

8. X. Li, L. Wu, Z. Liu, B. Hussain, W. C. Chong, K. M. Lau, and C. P. Yue, "Design and Characterization of Active Matrix LED Microdisplays With Embedded Visible Light Communication Transmitter," *J. Lightwave Technol.* **34**(14), 3449–3457 (2016).
9. M. S. Islam, R. X. Ferreira, X. He, E. Xie, S. Videv, S. Viola, S. Watson, N. Bamiedakis, R. V. Penty, I. H. White, A. E. Kelly, E. Gu, H. Haas, and M. D. Dawson, "Towards 10 Gb/s orthogonal frequency division multiplexing-based visible light communication using a GaN violet micro-LED," *Photonics Res.* **5**(2), A35–A43 (2017).
10. D. Tsonev, H. Chun, S. Rajbhandari, J. J. D. McKendry, S. Videv, E. Gu, M. Haji, S. Watson, A. E. Kelly, G. Faulkner, M. D. Dawson, H. Haas, and D. O'Brien, "A 3-Gb/s Single-LED OFDM-Based Wireless VLC Link Using a Gallium Nitride  $\mu$ LED," *IEEE Photonics Technol. Lett.* **26**(7), 637–640 (2014).
11. J. F. C. Carreira, E. Xie, R. Bian, C. Chen, J. J. D. McKendry, B. Guilhabert, H. Haas, E. Gu, and M. D. Dawson, "On-chip GaN-based dual-color micro-LED arrays and their application in visible light communication," *Opt. Express* **27**(20), A1517–A1528 (2019).
12. A. Rashidi, M. Monavarian, A. Aragon, A. Rishinaramangalam, and D. Feezell, "Nonpolar  $m$ -Plane InGaN/GaN Micro-Scale Light-Emitting Diode With 1.5 GHz Modulation Bandwidth," *IEEE Electron Device Lett.* **39**(4), 520–523 (2018).
13. R. Horng, H. Chien, K. Chen, W. Tseng, Y. Tsai, and F. Tarntair, "Development and Fabrication of AlGaInP-Based Flip-Chip Micro-LEDs," *IEEE J. Electron Devices Soc.* **6**, 475–479 (2018).
14. M.-C. Tseng, C.-L. Chen, N.-K. Lai, S.-I. Chen, T.-C. Hsu, Y.-R. Peng, and R.-H. Horng, "P-side-up thin-film AlGaInP-based light emitting diodes with direct ohmic contact of an ITO layer with a GaP window layer," *Opt. Express* **22**(S7), A1862–A1867 (2014).
15. J. F. C. Carreira, A. D. Griffiths, E. Xie, B. J. E. Guilhabert, J. Herrnsdorf, R. K. Henderson, E. Gu, M. J. Strain, and M. D. Dawson, "Direct integration of micro-LEDs and a SPAD detector on a silicon CMOS chip for data communications and time-of-flight ranging," *Opt. Express* **28**(5), 6909–6917 (2020).
16. M. Meitl, Z. Zhu, V. Kumar, K. Lee, X. Feng, Y. Huang, I. Adesida, R. Nuzzo, and J. Rogers, "Transfer printing by kinetic control of adhesion to an elastomeric stamp," *Nat. Mater.* **5**(1), 33–38 (2006).
17. H. Zhang and J. A. Rogers, "Recent Advances in Flexible Inorganic Light Emitting Diodes: From Materials Design to Integrated Optoelectronic Platforms," *Adv. Opt. Mater.* **7**(2), 1800936 (2019).
18. A. J. Trindade, B. Guilhabert, E. Y. Xie, R. Ferreira, J. J. D. McKendry, D. Zhu, N. Laurand, E. Gu, D. J. Wallis, I. M. Watson, C. J. Humphreys, and M. D. Dawson, "Heterogeneous integration of gallium nitride light-emitting diodes on diamond and silica by transfer printing," *Opt. Express* **23**(7), 9329–9338 (2015).
19. X. Lin, D. Liu, G. Lin, Q. Zhang, N. Gao, D. Zhao, R. Jia, Z. Zuo, and X. Xu, "Periodic indentation patterns fabricated on AlGaInP light emitting diodes and their effects on light extraction," *RSC Adv.* **4**(108), 63143–63146 (2014).
20. S. Franssila, *Introduction to Microfabrication* (John Wiley & Sons, Ltd, 2010).
21. R. P. Mildren, *Intrinsic Optical Properties of Diamond* (John Wiley & Sons, Ltd, 2013), , chap. 1, pp. 1–34.
22. M. Z. Afgani, H. Haas, H. Elgala, and D. Knipp, "Visible light communication using OFDM," in *2nd International Conference on Testbeds and Research Infrastructures for the Development of Networks and Communities, 2006. TRIDENTCOM 2006.*, (2006), pp. 6–134.
23. J. Armstrong and A. J. Lowery, "Power efficient optical OFDM," *Electron. Lett.* **42**(6), 370–372 (2006).
24. H. Haas, L. Yin, Y. Wang, and C. Chen, "What is LiFi?" *J. Lightwave Technol.* **34**(6), 1533–1544 (2016).
25. R. Bian, I. Tavakkolnia, and H. Haas, "15.73 Gb/s Visible Light Communication With Off-the-Shelf LEDs," *J. Lightwave Technol.* **37**(10), 2418–2424 (2019).
26. H. Chun, S. Rajbhandari, G. Faulkner, D. Tsonev, E. Xie, J. J. D. McKendry, E. Gu, M. D. Dawson, D. C. O'Brien, and H. Haas, "LED Based Wavelength Division Multiplexed 10 Gb/s Visible Light Communications," *J. Lightwave Technol.* **34**(13), 3047–3052 (2016).
27. Y. Wang, X. Huang, L. Tao, J. Shi, and N. Chi, "4.5-Gb/s RGB-LED based WDM visible light communication system employing CAP modulation and RLS based adaptive equalization," *Opt. Express* **23**(10), 13626–13633 (2015).
28. E. Xie, X. He, M. S. Islam, A. A. Purwita, J. J. D. McKendry, E. Gu, H. Haas, and M. D. Dawson, "High-Speed Visible Light Communication Based on a III-Nitride Series-Biased Micro-LED Array," *J. Lightwave Technol.* **37**(4), 1180–1186 (2019).